

Article

# Study of the Interactions of Bovine Serum Albumin with the New Anti-Inflammatory Agent 4-(1,3-Dioxo-1,3-dihydro-2*H*-isoindol-2-yl)-*N'*-(4-ethoxy-phenyl)methylidene]benzohydrazide Using a Multi-Spectroscopic Approach and Molecular Docking

Tanveer A. Wani <sup>1,\*</sup>, Ahmed H. Bakheit <sup>1</sup> , Abdul-Rahman A. Al-Majed <sup>1</sup> , Mashooq A. Bhat <sup>1</sup> and Seema Zargar <sup>2</sup>

<sup>1</sup> Department of Pharmaceutical Chemistry, College of Pharmacy, King Saud University, P.O. Box 2457, Riyadh 11451, Saudi Arabia; abujazz76@gmail.com (A.H.B.); almajed99@yahoo.com (A.-R.A.A.-M.); mabhat@ksu.edu.sa (M.A.B.)

<sup>2</sup> Department of Biochemistry, College of Science, King Saud University, P.O. Box 22452, Riyadh 11451, Saudi Arabia; szargar@ksu.edu.sa

\* Correspondence: twani@ksu.edu.sa; Tel.: +966-11-467-9841

Received: 22 June 2017; Accepted: 26 July 2017; Published: 27 July 2017

**Abstract:** The lipophilic derivative of thalidomide (4-(1,3-dioxo-1,3-dihydro-2*H*-isoindol-2-yl)-*N'*-(4-ethoxyphenyl)methylidene]benzohydrazide, **6P**) was synthesized to enhance its characteristics and efficacy. Earlier studies have proved the immunomodulatory and anti-inflammatory effects of **6P**. In this study the interaction between bovine serum albumin (BSA) and **6P** was studied using a multi-spectroscopic approach which included UV spectrophotometry, spectrofluorimetry and three dimensional spectrofluorometric and molecular docking studies. Static quenching was involved in quenching the fluorescence of BSA by **6P**, because a complex formation occurred between the **6P** and BSA. The binding constant decreased with higher temperature and was in the range of  $2.5 \times 10^5$ – $4.8 \times 10^3$  L mol<sup>-1</sup> suggesting an unstable complex at higher temperatures. A single binding site was observed and the site probe experiments showed site II (sub-domain IIIA) of BSA as the binding site for **6P**. The negative values of  $\Delta G^0$ ,  $\Delta H^0$  and  $\Delta S^0$  at (298/303/308 K) indicated spontaneous binding between **6P** and BSA as well as the interaction was enthalpy driven and van der Waals forces and hydrogen bonding were involved in the interaction. The docking results and the results from the experimental studies are complimentary to each other and confirm that **6P** binds at site II (sub-domain IIIA) of BSA.

**Keywords:** HSA; BSA; serum albumin; thalidomide; lipophilic thalidomide derivative; fluorescence; quenching; **6P**

## 1. Introduction

Thalidomide and its various derivatives are used as prophylactic drugs in the case of autoimmune diseases due to their immunomodulatory and anti-inflammatory properties [1]. Chemically thalidomide is ( $\alpha$ -*N*-phthalimidoglutarimide) and was indicated as a sedative in 1954, however due to its teratogenic effects it was withdrawn and later reintroduced and approved for use in nodosum leprosum and in multiple myeloma [2]. Recent studies have indicated the usefulness of thalidomide in prostate cancer, Crohn's disease, lupus erythematosus, chronic host-versus-graft disease, HIV-associated oral ulcers, rheumatoid arthritis and Behcet's disease [3–5]. In several animal studies it has been shown to suppress various inflammatory markers such as TNF- $\alpha$ , IL-1 $\beta$ , IL-6, and NO, thus relieving inflammation and

pain [6–9]. To overcome the teratogenic, peripheral neuropathic and other adverse events caused by thalidomide several structural analogues were synthesized and these exhibited less toxicity and were highly potent. Structural modification of thalidomide has produced potent inhibitors of TNF- $\alpha$  [10,11].

In a similar fashion the lipophilic thalidomide derivative (4-(1,3-dioxo-1,3-dihydro-2*H*-isoindol-2-yl)-*N'*-[(4-ethoxyphenyl)methylidene]benzohydrazide (**6P**, Figure 1) was synthesized by modifying the thiomorpholine group by introducing hydrophobic moieties to enhance its lipophilic characteristics and anti-inflammatory properties [12]. A decrease in the inflammation markers IL-6, IL-17, TNF- $\alpha$ , NF- $\kappa$ B, GTR, STAT-3, COX-2 and iNOS was observed after treatment with **6P** in a mouse model (lung inflammation) which was further corroborated by the histopathological studies. Anti-inflammatory mediators IL-10 and IL-4 showed an increase post-treatment with **6P** suggesting potent anti-inflammatory agent effect of **6P** in the carrageenan-induced lung inflammation. Further, histopathological examination also confirmed the potent anti-inflammatory effects of the compound **6P**. Compound **6P**, being a small molecule, has the capability to bind to various targets like transcription factor NF- $\kappa$ B p65, 1MY5 PDB-structure, etc., thus increasing its anti-inflammatory potential [12].

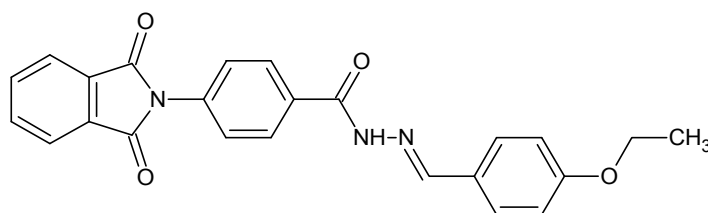


**Figure 1.** Chemical structure of the lipophilic thalidomide derivative (4-(1,3-dioxo-1,3-dihydro-2*H*-isoindol-2-yl)-*N'*-[(4-ethoxyphenyl)methylidene]benzohydrazide (**6P**).

Serum albumin (SA) is the major protein involved in the transport of drug ligands, thus affecting the ADME (absorption, distribution, metabolism and excretion) of these drugs [13–15]. Thus the first step in evaluation of the pharmacokinetics of these drug ligands is to investigate its affinity towards SA [16]. BSA being the model protein due to its structural resemblance to HSA and its low-cost and obtainability was used to study the interaction between the BSA and **6P**. The biophysical interaction of **6P** with BSA was studied using multi-spectroscopic studies along with molecular docking [15,17,18]. The study will provide a great insight regarding the pharmacokinetic behavior of the **6P** in-vivo.

## 2. Results and Discussion

### 2.1. Study of Conformational Changes in BSA with UV-Visible Spectroscopy

The structural changes and the complex formation within the **6P** and BSA was studied with the help of absorption spectroscopy [19]. The spectra of BSA alone as well as with increasing concentrations of **6P** are presented in the Figure 2. The band at 280 nm produced by the BSA represents the  $\pi \rightarrow \pi$  transition because of amino acids present in it. The absorption intensity of BSA increased post **6P** addition, indicating that the BSA molecules were associated with **6P** and formed a **6P**-BSA complex. Further, the maximum absorbance peak shifted slightly towards a lower wavelength. These two results, i.e., shifting of the maximum absorbance and an increase in the absorption intensity together evidently inferred the presence of an interaction between **6P** and BSA and also indicated a change in the conformation of BSA.

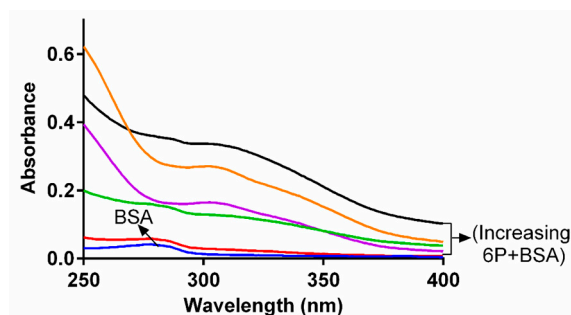


Figure 2. Spectra of BSA in presence and absence of 6P.

## 2.2. Fluorescence Quenching of BSA

In drug binding studies, fluorescence quenching methodology plays a very important role in exploration of the interaction between ligand and proteins [20]. The fluorescence spectra of BSA were obtained in absence and in the presence of different concentrations of 6P (Figure 3). A decrease in the FI of BSA was observed as the concentration of 6P was increased with a slight change in the  $\lambda$  emission of BSA. This alteration in the  $\lambda$  emission indicated a slight change in the fluorophore microenvironment during the interaction of 6P and BSA.

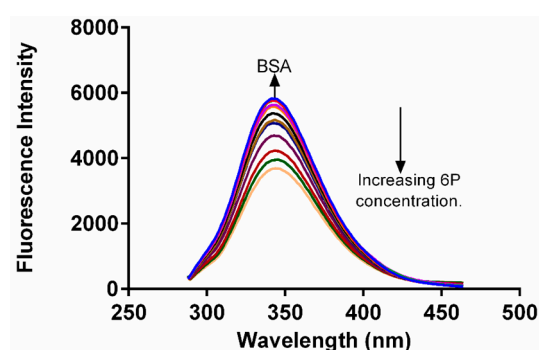


Figure 3. Spectra for fluorescence quenching of BSA in the presence and absence of 6P at 25 °C.

## 2.3. Analysis of Fluorescence Quenching and Mechanism

The two processes by which quenching can occur are static quenching and dynamic quenching. In the case of static quenching formation of a complex between the ligand and protein takes place and the complex formed is non-fluorescent in nature. In the case of dynamic quenching the fluorophore and the quencher interact with one another during the course of excitation. The static and dynamic quenching can also be differentiated on the basis of their dependence on temperature and viscosity. In addition to these two parameters they can also be distinguished from each other on the basis of their life time measurements. At higher temperatures in dynamic quenching there is an intensification of diffusion and collisional quenching resulting in a higher quenching constant. A similar increase in temperature in case of static quenching causes the reverse effect on the quenching constant. The mechanism of quenching involved can be determined with help of Stern-Volmer equation:

$$\frac{F}{F_0} = 1 + K_{sv}[Q] = 1 + K_q \tau_0 [Q] \quad (1)$$

In the above equation  $F$  and  $F_0$  represent the FI of BSA in presence and absence of 6P;  $K_{sv}$ ,  $K_q$ ,  $[Q]$  represent the Stern-Volmer constant, bimolecular quenching rate constant and quencher concentration respectively;  $\tau_0$  is the lifetime of fluorophore in absence of quencher and is valued to be  $10^{-8}$  in case of biopolymers. The obtained  $K_{sv}$  and  $K_q$  values are presented in Table 1 (Figure 4A).

In addition to  $K_{SV}$ , bimolecular quenching rate constant also assists to determine the type of quenching involved in the process.

**Table 1.** Stern–Volmer quenching constants ( $K_{SV}$ ) and bimolecular quenching rate constant ( $K_q$ ) for the binding of **6P** to BSA at three variable temperatures.

T (K)	R	$K_{sv}$ ( $L \cdot mol^{-1}$ )	$K_q$ ( $L \cdot mol^{-1} \cdot s^{-1}$ )
298	0.9934	$2.73 \times 10^4$	$2.73 \times 10^{12}$
303	0.9957	$3.02 \times 10^4$	$3.02 \times 10^{12}$
308	0.9913	$3.20 \times 10^4$	$3.20 \times 10^{12}$

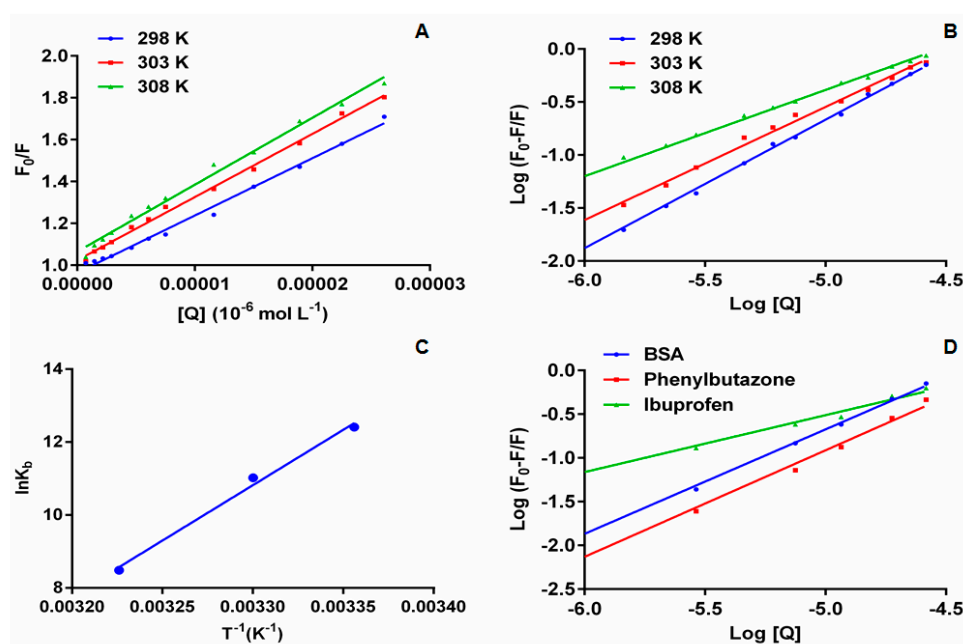


**Figure 4.** (A): The stern–Volmer curves for the quenching of BSA by **6P** at 298/303/308 K; (B): The plot of  $\log[(F_0 - F)/F]$  versus  $\log[Q]$  for quenching process of **6P** with BSA at 298/303/3008 K; (C): Van't Hoff plots for the binding interaction of **6P** with BSA; (D): The plot of  $\log[(F_0 - F)/F]$  versus  $\log[Q]$  for quenching process of **6P** with BSA in presence of site markers phenylbutazone and ibuprofen at 298 K.

An increase in the  $K_{sv}$  and  $K_q$  values was observed indicating the possibility of involvement of dynamic quenching. The rate constant for scattering collision quenching can attain a maximum value of  $2 \times 10^{10} L M^{-1} S^{-1}$ . The obtained  $K_q$  values are much higher than  $2 \times 10^{10} L M^{-1} S^{-1}$  indicating the formation of non-fluorescent complex (static quenching) amongst **6P** and BSA.

Although there is a difference between the two quenching mechanisms, the interaction of **6P** with BSA can be further explained from the UV absorption spectra of BSA in presence of **6P**. In the case where dynamic quenching were involved there would had been no change in the absorption spectrum of BSA in the presence of **6P** as only the excitation state of the quencher is affected, with no effect on the UV-absorption spectra of BSA, whereas in the case of static quenching formation of a complex occurs between the ligand and the protein causing changes in the UV-absorption spectra of BSA in the presence of ligands. According to the UV spectra complex formation (i.e., static quenching) occurred between BSA and **6P** which was further corroborated with the obtained high  $K_q$  values [20–23].

#### 2.4. Binding Constant and Binding Modes

To determine the binding constant ( $K_b$ ) and binding site number ( $n$ ) double log regression curve is used (Figure 4B) [23]. It is assumed that one or more than one binding sites are available on the

protein molecule to bind the ligand. The  $K_b$  and  $n$  are calculated from the intercept and slope of the plotted double log regression curve (Table 2):

$$\log \frac{(F_0 - F)}{F} = \log K_b + n \log [Q] \quad (2)$$

**Table 2.** Binding and thermodynamic parameters of binding between **6P** and BSA.

T (K)	R	$K_b$ (L·mol <sup>-1</sup> )	n	$\Delta G$ (kJ·mol <sup>-1</sup> )	$\Delta H$ (kJ·mol <sup>-1</sup> )	$\Delta S$ (J·mol <sup>-1</sup> ·K <sup>-1</sup> )
298	0.9980	$2.5 \times 10^5$	1.21	-31.01	-253	-744
303	0.9955	$6.2 \times 10^4$	1.06	-27.29		
308	0.9940	$4.8 \times 10^3$	0.81	-22.08		

The strength of the binding interaction is inferred from the values of  $K_b$ —the higher the value of  $K_b$  the stronger the binding between the protein and the ligand. The results show a decrease in the  $K_b$  values with an increase in temperature, demonstrating the instability of the **6P**-BSA complex at higher temperatures. It also suggests that static quenching is involved in the interaction between **6P** and BSA. The number of binding sites involved in the interaction of **6P** and BSA at all the studied temperatures were approximate equal to 1. A correlation coefficient ( $r^2$ ) of >0.99 at all the three studied temperatures indicates that the interaction between **6P** and BSA followed a binding model based on the double log regression method.

Further, phenylbutazone and ibuprofen were taken as site-specific probes to locate the binding site I and II of BSA, respectively, and their interaction with **6P**. To obtain this varied concentrations of **6P** were added to fixed concentrations of BSA protein and site probe marker. The fluorescence spectra of the resulting solutions were obtained at room temperature with an excitation wavelength of 280 nm. The deviations in the fluorescence spectra were utilized to obtain the binding constants (Figure 4C). For the **6P**-BSA-phenylbutazone system the binding constant was found out to be  $1.26 \times 10^5$  L·mol<sup>-1</sup> and for the **6P**-BSA-ibuprofen system the binding constant was found to be  $5.49 \times 10^2$  L·mol<sup>-1</sup>. These binding constants when compared to the **6P**-BSA system  $2.50 \times 10^5$  L·mol<sup>-1</sup> showed a remarkable decrease in the presence of ibuprofen whereas the  $K_b$  values showed little effect in the presence of phenylbutazone. These results indicate site II (sub-domain IIIA) as the binding site for **6P** [24].

### 2.5. Thermodynamic Parameters and Binding Forces

Drugs bind to protein molecules with the help of different types of binding forces, including van der Waals forces, hydrogen bonding, electrostatic interactions and hydrophobic interactions. Van't Hoff's equation is used to obtain the thermodynamic parameters. The signs of these forces (positive or negative) and the amount of these forces helps in determination of types of interaction involved within the ligand and the protein. Van't Hoff equation is given as follows:

$$\ln K_b = -\frac{\Delta H^0}{RT} + \frac{\Delta S^0}{R} \quad (3)$$

$$\Delta G^0 = \Delta H^0 - T\Delta S^0 = -RT \ln K_b \quad (4)$$

where  $\Delta G^0$ ,  $\Delta H^0$  and  $\Delta S^0$  represent the change Gibbs free energy, enthalpy and entropy, respectively, and  $R$  and  $K_b$  represent the universal gas constant and binding constant, respectively. The negative sign of the values for  $\Delta H^0$  and  $\Delta S^0$  represents the contribution of van der Waals forces and/or hydrogen bonding. The positive values for  $\Delta H^0$  and  $\Delta S^0$  represent hydrophobic interactions. If the value of  $\Delta H^0$  approaches zero and a compound has a positive  $\Delta S^0$  the involvement of electrostatic forces is suggested [25,26]. The van't Hoff plot for BSA and **6P** is represented in Figure 4D and the values for  $\Delta G^0$ ,  $\Delta H^0$  and  $\Delta S^0$  are presented in Table 2. (−)  $\Delta G^0$  indicates that BSA-**6P** binding was spontaneous. The calculated values for  $\Delta H^0$  and  $\Delta S^0$  were negative (−) indicating that the interaction between **6P** and

BSA was enthalpy driven with unfavorable entropy and van der Waals forces and hydrogen bonding play main roles in the **6P** and BSA interaction.

### 2.6. Synchronous Fluorescence Spectroscopy of BSA and **6P** Complex

Synchronous fluorescence spectroscopy (SFS) was used to study the microenvironment of the formed complex due to the **6P**-BSA interaction. SFS acts as an efficient tool to check the chromophore micro-environment [27]. The evidence regarding the tyrosine and tryptophan residue micro-environment is generated using scanning intervals of  $\Delta\lambda = 15$  nm and  $\Delta\lambda = 60$  nm, respectively. A shift in the emission wavelength of BSA suggests a change in the micro-environmental polarity of either tyrosine or tryptophan or both. The SFS of BSA were obtained without and with different concentrations of **6P** at both  $\Delta\lambda = 15$  nm and  $\Delta\lambda = 60$  nm (Figure 5). A shift of 1 nm in the emission wavelength was observed at  $\Delta\lambda = 60$  nm. This shift indicates a change in the micro-environment of tryptophan residue of BSA upon interaction with **6P**.

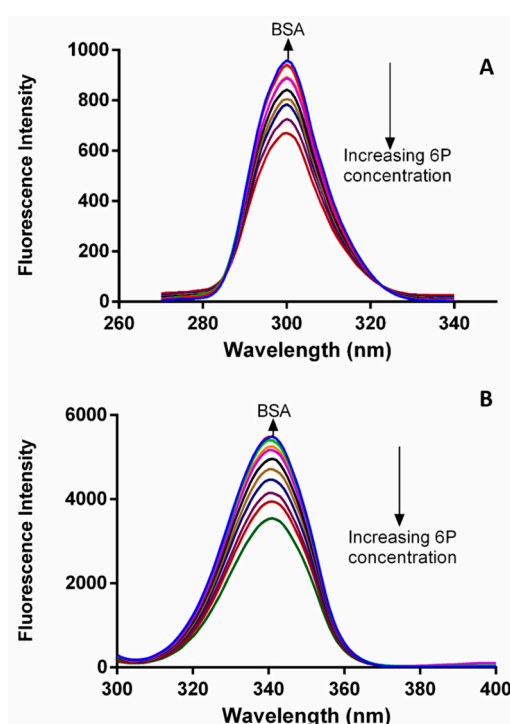


**Figure 5.** Synchronous fluorescence spectroscopy spectra of BSA at 298 K (A)  $\Delta\lambda = 15$  nm and (B)  $\Delta\lambda = 60$  nm.

The 3D (3-dimensional) spectra for BSA (Figure 6) were obtained with and without **6P** [28]. Peak 2 ( $\lambda_{\text{ex}}/\lambda_{\text{em}}$ : 280.0/344.0 nm) represents the presence of tryptophan and tyrosine residues and shows a decrease in the FI post **6P** addition. Peak 1 ( $\lambda_{\text{ex}}/\lambda_{\text{em}}$ : 234.0/344.0 nm) represents the polypeptides present in the BSA and is formed due to  $\pi$ - $\pi^*$  transitions in the polypeptide structures present in BSA. A sharp decrease in the FI is observed post **6P** addition. Further, the contour plot shows sparse spectra in presence of **6P** compared to BSA alone, suggesting conformational changes in BSA post **6P** interaction.

### 2.7. Molecular Simulation Studies

To extract more information regarding the BSA-**6P** interaction docking studies were performed. The most favored binding site and the binding mode were determined using docking analysis. The two ligand binding sites (Site I and Site II) present on the BSA molecule characterize the hydrophobic grooves present in sub-domains IIA and IIIA, respectively.



### 3. Materials and Methods

#### 3.1. Chemical and Reagents

BSA was purchased from Sisco Research Laboratories (Mumbai, India). **6P** was synthesized in-house in the Medicinal Chemistry Department (m.p.: 248–250 °C; IR (KBr):  $\nu$  max/cm<sup>-1</sup>: 3420 (CONH), 2927 (N=CH), 1739 (C=O); <sup>1</sup>H-NMR (DMSO-*d*<sub>6</sub>)  $\delta$  ppm: 1.3 (3H, t, CH<sub>3</sub>), 4.0 (2H, q, *J* = 5.5 Hz, -OCH<sub>2</sub>), 7.0–8.0 (12H, m, Ar-H), 8.4 (1H, s, N=CH), 11.8 (1H, s, CONH, D<sub>2</sub>O exchg.); <sup>13</sup>C-NMR (DMSO-*d*<sub>6</sub>)  $\delta$  ppm: 15.0, 63.7, 115.2, 124.0, 127.1, 127.5, 127.7, 128.6, 128.8, 129.1, 129.2, 131.9, 135.1, 135.3, 148.4, 162.8, 167.2; ESI mass (*m/z*): 412.10 [M – 1]<sup>+</sup> (calculated 413.42)). Phenylbutazone and ibuprofen was procured by from the National Scientific Company (Riyadh, Saudi Arabia). All the chemicals used for the study were of analytical grade. Phosphate buffer with pH 7.4 was used for the preparation of 1.5  $\mu$ M BSA standard solution. **6P** stock solution was prepared by dissolving 5 mg in 500  $\mu$ L dimethyl sulphoxide and the volume was made up with phosphate buffer to get a concentration of  $2.3 \times 10^{-3}$  M. The working standards for **6P** ranged between  $1.45 \times 10^{-6}$  and  $5.2 \times 10^{-5}$  M were prepared using the stock. The site marker stocks phenylbutazone and ibuprofen were prepared in methanol and dilutions for them were made with phosphate buffer. An Elga Purelab system (High Wycombe, UK) was used to obtain type IV water for the preparation of solutions.

#### 3.2. UV Spectra Measurements

Spectrophotometric measurements were carried using a UV-1800 spectrophotometer (Shimadzu, Kyoto, Japan). These UV spectra were obtained for BSA alone and with variable concentrations of **6P**. All the measurements were carried out at room temperature.

#### 3.3. Fluorescence Measurements

Fluorimetric spectra were obtained using a FP-8200 spectrofluorimeter (JASCO, Cremella, Italy). The spectra were obtained at excitation/emission wavelength of 280/340 nm respectively at temperatures of (298\303\308 K). The standard solutions were prepared by mixing fixed concentration of  $1.5 \times 10^{-6}$  M BSA solution in (1:1) *v/v* ratio with varied concentration  $1.45 \times 10^{-6}$  and  $5.2 \times 10^{-5}$  M of **6P** in 10 mL volumetric flasks and the final concentrations obtained for measuring the spectra were  $0.75 \times 10^{-6}$  M for BSA and  $7.26 \times 10^{-7}$  and  $2.6 \times 10^{-5}$  M for **6P**. The spectral measurement was repeated thrice and the final reading was the mean of the three experiments performed. The following equation was used to correct the inner filter effect of the fluorescence intensity.

$$F_{\text{COR}} = F_{\text{OBS}} \times e^{(A_{\text{EX}} + A_{\text{EM}})/2} \quad (5)$$

In the above equation  $F_{\text{COR}}$  represents the corrected fluorescence and  $F_{\text{OBS}}$  represents the observed fluorescence.  $A_{\text{EX}}$  represents the absorption by **6P** at excitation wavelength and the  $A_{\text{EM}}$  represents the **6P** absorption at emission wavelength. Since there is a possibility that the excitation and the emission wavelength can lie in the UV-absorption region, thus making it important to correct the inner filter effect.

#### 3.4. Synchronous Fluorescence (SF) Measurement

A JASCO spectrofluorimeter was used for obtaining the synchronous fluorescence data. The data was obtained at room temperature using increasing concentrations of **6P**. The scanning intervals used for the analysis were  $\Delta\lambda = 15$  nm and  $\Delta\lambda = 60$  nm which correspond to the characteristics of tyrosine and tryptophan residues.

#### 3.5. Molecular Docking

Molecular docking procedures provide a platform to analyze the interactions between ligands and proteins and support the experimental results. Docking analysis of the complex of **6P** and BSA

was performed to observe the interaction of **6P** at the active binding site of BSA with the Molecular Operating Environment (MOE) suite docking software. For the docking analysis the crystalline structure of BSA was obtained from Protein Data Bank (<http://www.rcsb.org>) whereas the structure of **6P** was drawn inside the MOE software itself. The best configuration of BSA with **6P** was selected on the basis of RMSD (root mean square deviation) parameters.

#### 4. Conclusions

**6P** being a promising anti-inflammatory drug was investigated for its interactions with the protein BSA in-vitro. **6P** was found to interact with BSA at site II in the subdomain IIIA of the BSA molecule. The complex formation was further explained with help of fluorescence quenching studies, spectrophotometric experiments, SFS, three dimensional fluorescence data and molecular modelling. A single binding site was observed on BSA to interact with **6P**. The complex formed between **6P** and BSA was enthalpy driven, with van der Waals forces and hydrogen bonding interactions playing the main roles. Serum albumin acts a carrier of drug ligands, thus, the results from our study will help in predicting the distribution and metabolism of **6P** in vivo, which would help us to further understand the pharmacodynamics of the **6P**. In addition this study provided vital information regarding the pharmacology and biochemistry of **6P** at the screening stage.

**Acknowledgments:** The authors would like to extend their sincere appreciation to the Deanship of Scientific Research, King Saud University, for funding the research group No. RG-1438-042.

**Author Contributions:** T.A.W. and S.Z. designed the study. A.H.B., A.-R.A.A.-M. participated in conduct of experiments. AHB carried out the molecular modeling analysis. MAB provided the materials. T.W., A.-R.A.A.-M. and S.Z. analyzed the results and wrote the manuscript. All authors read and approved the final manuscript.

**Conflicts of Interest:** The authors declare that they have no competing interests.

#### References

1. Sampaio, E.P.; Sarno, E.N.; Galilly, R.; Cohn, Z.A.; Kaplan, G. Thalidomide selectively inhibits tumor necrosis factor  $\alpha$  production by stimulated human monocytes. *J. Exp. Med.* **1991**, *173*, 699–703. [[CrossRef](#)] [[PubMed](#)]
2. Melchert, M.; List, A. The thalidomide saga. *Int. J. Biochem. Cell Biol.* **2007**, *39*, 1489–1499. [[CrossRef](#)] [[PubMed](#)]
3. Teo, S.K. Properties of thalidomide and its analogues: Implications for anticancer therapy. *AAPS J.* **2005**, *7*, E14–E19. [[CrossRef](#)] [[PubMed](#)]
4. Hashimoto, Y. Thalidomide as a multi-template for development of biologically active compounds. *Arch. Der Pharm.* **2008**, *341*, 536–547. [[CrossRef](#)] [[PubMed](#)]
5. Chen, M.; Doherty, S.D.; Hsu, S. Innovative uses of thalidomide. *Dermatol. Clin.* **2010**, *28*, 577–586. [[CrossRef](#)] [[PubMed](#)]
6. Mazzon, E.; Muià, C.; Di Paola, R.; Genovese, T.; De Sarro, A.; Cuzzocrea, S. Thalidomide treatment reduces colon injury induced by experimental colitis. *Shock* **2005**, *23*, 556–564. [[PubMed](#)]
7. Amirshahrokhi, K. Anti-inflammatory effect of thalidomide in paraquat-induced pulmonary injury in mice. *Int. Immunopharmacol.* **2013**, *17*, 210–215. [[CrossRef](#)] [[PubMed](#)]
8. Goli, V. Does thalidomide have an analgesic effect? Current status and future directions. *Curr. Pain Headache Rep.* **2007**, *11*, 109–114. [[CrossRef](#)] [[PubMed](#)]
9. Rocha, A.C.; Fernandes, E.S.; Quintão, N.L.; Campos, M.M.; Calixto, J.B. Relevance of tumour necrosis factor- $\alpha$  for the inflammatory and nociceptive responses evoked by carrageenan in the mouse paw. *Br. J. Pharmacol.* **2006**, *148*, 688–695. [[CrossRef](#)] [[PubMed](#)]
10. Niwayama, S.; Turk, B.E.; Liu, J.O. Potent inhibition of tumor necrosis factor- $\alpha$  production by tetrafluorothalidomide and tetrafluorophthalimides. *J. Med. Chem.* **1996**, *39*, 3044–3045. [[CrossRef](#)] [[PubMed](#)]
11. Muller, G.W.; Corral, L.G.; Shire, M.G.; Wang, H.; Moreira, A.; Kaplan, G.; Stirling, D.I. Structural modifications of thalidomide produce analogs with enhanced tumor necrosis factor inhibitory activity 1. *J. Med. Chem.* **1996**, *39*, 3238–3240. [[CrossRef](#)] [[PubMed](#)]
12. Bhat, M.A.; Al-Omar, M.A.; Ansari, M.A.; Zoheir, K.M.; Imam, F.; Attia, S.M.; Bakheet, S.A.; Nadeem, A.; Korashy, H.M.; Voronkov, A. Design and synthesis of *n*-arylpthalimides as inhibitors of glucocorticoid-induced tnfr receptor-related protein, proinflammatory mediators, and cytokines in carrageenan-induced lung inflammation. *J. Med. Chem.* **2015**, *58*, 8850–8867. [[CrossRef](#)] [[PubMed](#)]

13. Wani, T.A.; Zargar, S.; Ahmad, A. Ultra-performance liquid chromatography tandem mass spectrometric method development and validation for determination of neratinib in human plasma. *S. Afr. J. Chem.* **2015**, *68*, 93–98. [[CrossRef](#)]
14. Wani, T.A.; Samad, A.; Sharma, P.; Tandon, M.; Paliwal, J. Determination of interchangeability of different brands of diclofenac sodium sustained release tablets in healthy subjects using pharmacokinetic end points. *Lett. Drug Des. Discov.* **2009**, *6*, 629–636. [[CrossRef](#)]
15. Wani, T.A.; Bakheit, A.H.; Zargar, S.; Hamidaddin, M.A.; Darwish, I.A. Spectrophotometric and molecular modelling studies on in vitro interaction of tyrosine kinase inhibitor linifanib with bovine serum albumin. *PLoS ONE* **2017**, *12*, e0176015. [[CrossRef](#)] [[PubMed](#)]
16. Iqbal, M.; Bhat, M.A.; Raish, M.; Ezzeldin, E. Determination of (4-(1,3-dioxo-1,3-dihydro-2H-isoindol-2-yl)-N'-[(4-ethoxyphenyl)methylidene]benzohydrazide, a novel anti-inflammatory agent, in biological fluids by UPLC-MS/MS: Assay development, validation and in vitro metabolic stability study. *Biomed. Chromatogr.* **2017**. [[CrossRef](#)] [[PubMed](#)]
17. Khorsand Ahmadi, S.; Mahmoodian Moghadam, M.; Mokaberi, P.; Reza Saberi, M.; Chamani, J. A comparison study of the interaction between  $\beta$ -lactoglobulin and retinol at two different conditions: Spectroscopic and molecular modeling approaches. *J. Biomol. Struct. Dyn.* **2015**, *33*, 1880–1898. [[CrossRef](#)] [[PubMed](#)]
18. Marouzi, S.; Rad, A.S.; Beigoli, S.; Baghaee, P.T.; Darban, R.A.; Chamani, J. Study on effect of lomefloxacin on human holo-transferrin in the presence of essential and nonessential amino acids: Spectroscopic and molecular modeling approaches. *Int. J. Biol. Macromol.* **2017**, *97*, 688–699. [[CrossRef](#)] [[PubMed](#)]
19. Moriyama, Y.; Ohta, D.; Hachiya, K.; Mitsui, Y.; Takeda, K. Fluorescence behavior of tryptophan residues of bovine and human serum albumins in ionic surfactant solutions: A comparative study of the two and one tryptophan (s) of bovine and human albumins. *J. Protein Chem.* **1996**, *15*, 265–272. [[CrossRef](#)] [[PubMed](#)]
20. Lackowicz, J. *Principle of Fluorescence Spectroscopy*; Springer Science and Business Media: Spring Street, NY, USA, 2006; Volume 13, pp. 278–327.
21. Lakowicz, J.R.; Weber, G. Quenching of fluorescence by oxygen. Probe for structural fluctuations in macromolecules. *Biochemistry* **1973**, *12*, 4161–4170. [[CrossRef](#)] [[PubMed](#)]
22. Hu, Y.J.; Liu, Y.; Wang, J.B.; Xiao, X.H.; Qu, S.S. Study of the interaction between monoammonium glycyrrhizinate and bovine serum albumin. *J. Pharm. Biomed. Anal.* **2004**, *36*, 915–919. [[CrossRef](#)] [[PubMed](#)]
23. Shahabadi, N.; Hadidi, S.; Feizi, F. Study on the interaction of antiviral drug 'Tenofovir' with human serum albumin by spectral and molecular modeling methods. *Spectrochim. Acta A Mol. Biomol. Spectrosc.* **2015**, *138*, 169–175. [[CrossRef](#)] [[PubMed](#)]
24. Shi, J.h.; Pan, D.Q.; Jiang, M.; Liu, T. T.; Wang, Q. In vitro study on binding interaction of quinapril with bovine serum albumin (BSA) using multi-spectroscopic and molecular docking methods. *J. Biomol. Struct. Dyn.* **2016**, 1–13. [[CrossRef](#)] [[PubMed](#)]
25. Ni, Y.; Liu, G.; Kokot, S. Fluorescence spectrometric study on the interactions of isoprocarb and sodium 2-isopropylphenate with bovine serum albumin. *Talanta* **2008**, *76*, 513–521. [[CrossRef](#)] [[PubMed](#)]
26. Ross, P.D.; Subramanian, S. Thermodynamics of protein association reactions: Forces contributing to stability. *Biochemistry* **1981**, *20*, 3096–3102. [[CrossRef](#)] [[PubMed](#)]
27. Albert, D.H.; Tapang, P.; Magoc, T.J.; Pease, L.J.; Reuter, D.R.; Wei, R.Q.; Li, J.; Guo, J.; Bousquet, P.F.; Ghoreishi-Haack, N.S. Preclinical activity of abt-869, a multitargeted receptor tyrosine kinase inhibitor. *Mol. Cancer Ther.* **2006**, *5*, 995–1006. [[CrossRef](#)] [[PubMed](#)]
28. Meti, M.D.; Nandibewoor, S.T.; Joshi, S.D.; More, U.A.; Chimatadar, S.A. Multi-spectroscopic investigation of the binding interaction of fosfomycin with bovine serum albumin. *J. Pharm. Anal.* **2015**, *5*, 249–255. [[CrossRef](#)]

**Sample Availability:** Samples of the compound 4-(1,3-Dioxo-1,3-dihydro-2H-isoindol-2-yl)-N'-[(4-ethoxy-phenyl)methylidene]benzohydrazine are available from the authors.



© 2017 by the authors. Licensee MDPI, Basel, Switzerland. This article is an open access article distributed under the terms and conditions of the Creative Commons Attribution (CC BY) license (<http://creativecommons.org/licenses/by/4.0/>).